ORIGINAL ARTICLE

ETRI Journal WILEY

Effective identification of dominant fully absorbing sets for Raptor-like LDPC codes

Woncheol Cho 🔗 | **Chanho Yoon** | **Kapseok Chang** | **Young-Jo Ko**

Mobile Communication Research Division, Electronics and Telecommunications Research Institute, Daejeon, Republic of Korea

Correspondence
Woncheol Cho, Mobile Communication Research Division, Electronics and Telecommunications Research Institute, Daejeon, Republic of Korea.
Email: woncheol@etri.re.kr

Abstract

The error-rate floor of low-density parity-check (LDPC) codes is attributed to the trapping sets of their Tanner graphs. Among them, fully absorbing sets dominantly affect the error-rate performance, especially for short blocklengths. Efficient methods to identify the dominant trapping sets of LDPC codes were thoroughly researched as exhaustively searching them is NP-hard. However, the existing methods are ineffective for Raptor-like LDPC codes, which have many types of trapping sets. An effective method to identify dominant fully absorbing sets of Raptor-like LDPC codes is proposed. The search space of the proposed algorithm is optimized into the Tanner subgraphs of the codes to afford time-efficiency and search-effectiveness. For 5G New Radio (NR) base graph (BG) 2 LDPC codes for short blocklengths, the proposed algorithm finds more dominant fully absorbing sets within one seventh of the computation time of the existing search algorithm, and its search-effectiveness is verified using importance sampling. The proposed method is also applied to 5G NR BG1 LDPC code and Advanced Television Systems Committee 3.0 type A LDPC code for large blocklengths.

KEYWORDS
5G NR LDPC code, ATSC 3.0 LDPC code, error-rate floor, fully absorbing set, Raptor-like LDPC code, trapping set

1 | INTRODUCTION

Ultra-reliable low-latency communication (URLLC) is one of 5G usage scenarios toward industries such as factory automation and power distribution. As machine-type data are typically several hundred bits long for mission-critical URLLC applications, channel codes with high error-correcting capabilities for short blocklengths have been explored. Low-density parity-check (LDPC) codes are considered as one of the appealing codes for URLLC because of their competitive performances in the short blocklength regime [1,2]. Recently, a design paradigm of quasicyclic (QC) Raptor-like LDPC codes was adopted as 5G New Radio (NR) channel codes for user data in enhanced mobile broadband (eMBB) usage scenario [2–5], and Advanced Television Systems Committee (ATSC) 3.0 channel codes for very low code rates [6,7]. QC-Raptor-like LDPC codes enable simple encoding implementation supporting rate compatibility [8,9]. In addition, a large degree of parallelism enables high-throughput encoding and decoding architectures [10,11].

However, the error-rate floor of LDPC codes in the short blocklength regime can hinder the achievement of link reliability on the order of $(1 - 10^{-7})$ or more. In an LDPC code, a codeword can be decoded by a near-optimal iterative decoder [12,13], where the optimality criterion is maximum a posteriori. If the independence among extrinsic information is broken by cycles inherent in the Tanner graph of the code during subsequent decoding iterations, the decoder can fall into a local optimum called a trapping set (TS). The error-rate floor of the code is attributed to the TSs inherent in its Tanner graph, especially for short blocklengths [14]. Among these TSs, small fully absorbing sets (FASs) are known as the most dominant causes of the error floor [15]. Here, the term "dominant" is used to mean more detrimental to the error floor, similar to the definition in [16].

Various results on efficiently finding dominant TSs of LDPC codes have been reported, considering that exhaustively searching TSs is NP-hard. The algorithm proposed in Karimi and Banihashemi [16] efficiently searches elementary TSs by utilizing the structural property that these TSs are unions of short cycles. A simulation-based method was proposed to identify TSs defined as a set of error bits when a decoder fails because of an error impulse [17]. Recently, a method to identify small elementary absorbing sets (ASs) for 5G NR LDPC codes was introduced [18]. The efficient exhaustive algorithm proposed in Hashemi and Banihashemi [19] is effective in identifying elementary TSs in the QC-LDPC codes of 802.11n [20] and 802.16e [21]. However, the existing methods can fall into a local optimum when finding the dominant TSs of Raptor-like LDPC codes, which have various types of TSs, because of the highest-rate codes and degree-1 variable nodes. In this paper, an effective method is proposed to identify dominant FASs for Raptor-like LDPC codes. The search space is optimized to Raptor-like LDPC codes, and search process is decoupled, thereby achieving both time-efficiency and search-effectiveness. To the best of our knowledge, this is the first paper to present FAS enumerators of 5G NR LDPC codes and ATSC 3.0 type A LDPC codes.

The rest of this paper is organized as follows. Section 2 introduces the preliminaries regarding Raptor-like LDPC codes, dominant FASs, and the importance sampling method [22]. The dominant FAS search method for Raptor-like LDPC codes is proposed in Section 3. In Section 4, the FAS enumerators of 5G NR LDPC codes and ATSC 3.0 type A LDPC code are presented. The proposed method can identify more dominant FASs within a shorter computation time than the existing search algorithm. In Section 4.1, the dominance of the FASs found by the proposed method is verified by error-rate estimation with importance sampling. In addition, the effects of 5G NR rate-matching schemes in the short blocklength regime [5,18,23] are discussed in Section 4.2 based on the observed FAS enumerators. Finally, Section 5 concludes the paper.

2 | PRELIMINARIES

2.1 | Raptor-like LDPC codes

In an (N, K) Raptor-like LDPC code, an $M \times N$ parity-check matrix $\mathbf{H} = (h_{ji})$ can be partitioned into submatrices as [3]

$$\mathbf{H} = \begin{bmatrix} \mathbf{H}_{\mathrm{HRC}} & \mathbf{O} \\ \mathbf{H}_{\mathrm{IRC}} & \mathbf{I} \end{bmatrix}, \tag{1}$$

where $\mathbf{H}_{\mathrm{HRC}}$ is $M_1 \times (K + M_1)$ parity-check matrix of the highest-rate code (HRC); $\mathbf{H}_{\mathrm{IRC}}$ is $M_2 \times (K + M_1)$ parity-check matrix of the incremental redundancy code (IRC); $\mathbf{O}$ is $M_1 \times M_2$ all-zeros matrix; $\mathbf{I}$ is $M_2 \times M_2$ identity matrix; and $M = N - K = M_1 + M_2$. An example of a Tanner graph of a Raptor-like LDPC code is shown in Figure 1. The Raptor-like LDPC code can be deemed as a serial concatenation of an outer HRC and an inner IRC or a low-density generator matrix (LDGM) code. Suppose an input message $\mathbf{u}$ is encoded into codeword $\mathbf{c} = [\mathbf{u} \ \mathbf{p}_1 \ \mathbf{p}_2]$. In the outer systematic HRC, $\mathbf{u}$ is encoded into $[\mathbf{u} \ \mathbf{p}_1]$. In the inner IRC or LDGM code, $\mathbf{p}_2$ is computed by the following equation:

$$\mathbf{p}_2 = [\mathbf{u} \ \mathbf{p}_1] \cdot \mathbf{H}_{\mathrm{IRC}}^{\mathrm{T}}, \tag{2}$$

which is essentially the exclusive-OR operation of bits encoded by the outer HRC. Therefore, the Raptor-like LDPC code enables simple encoding implementation supporting incremental redundancy hybrid automatic repeat request (IR-HARQ). Besides, as decoding complexity is proportional to the length of the codeword, the decoding throughput can be enhanced at higher code rates [11].
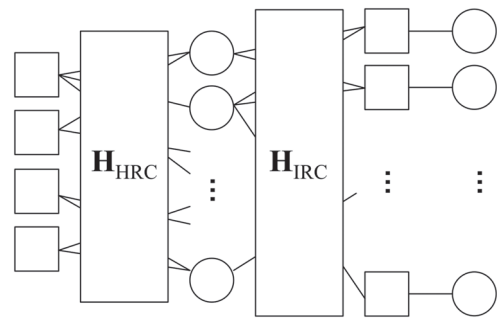

FIGURE 1 Sketch of Tanner graph for Raptor-like low-density parity-check (LDPC) code

A design paradigm of QC-Raptor-like LDPC codes with lifting size Z was adopted as the 5G NR LDPC code and ATSC 3.0 type A LDPC code. In an (N, K) 5G NR LDPC code with $N = n \cdot Z$ and $K = k \cdot Z$, the parity-check matrix of the HRC follows the approximate lower triangular form represented as [8]

$$\mathbf{H}_{\mathrm{HRC}} = \begin{bmatrix} \mathbf{A} & \mathbf{B} & \mathbf{T} \\ \mathbf{C} & \mathbf{D} & \mathbf{E} \end{bmatrix}, \tag{3}$$

where the sizes of $\mathbf{A}$, $\mathbf{B}$, $\mathbf{C}$, $\mathbf{D}$, and $\mathbf{E}$ are $3Z \times K, 3Z \times Z, Z \times K, Z \times Z$, and $Z \times 3Z$, respectively, and $\mathbf{T}$ is a $3Z \times 3Z$ lower triangular matrix. Let the base matrix be the parity-check matrix of a protograph. The base matrix corresponding to the HRC parity variable nodes of 5G NR base graph (BG) 1 and BG2 LDPC codes can be represented as

$$\begin{bmatrix} 1 & 1 & 0 & 0 \\ 1 & 1 & 1 & 0 \\ 0 & 0 & 1 & 1 \\ 1 & 0 & 0 & 1 \end{bmatrix}, \begin{bmatrix} 1 & 1 & 0 & 0 \\ 0 & 1 & 1 & 0 \\ 1 & 0 & 1 & 1 \\ 1 & 0 & 0 & 1 \end{bmatrix}, \tag{4}$$

respectively. A dual-diagonal-like accumulate structure in (4) was adopted in 802.11n [20], providing benefits in terms of error-rate performance and encoding complexity [8,9]. In an (N, K) ATSC 3.0 type A LDPC code with $N = n \cdot Z$ and $K = k \cdot Z$, the base matrix corresponding to the parity variable nodes of HRC is given by

$$\begin{bmatrix} 1 & 0 & 0 & \dots & 0 & 1 \\ 1 & 1 & 0 & \dots & 0 & 0 \\ 0 & 1 & 1 & \dots & 0 & 0 \\ \vdots & \vdots & \vdots & \ddots & \vdots & \vdots \\ 0 & 0 & 0 & \dots & 1 & 1 \end{bmatrix}. \tag{5}$$

The lifting size Z is fixed to 360, and the size of the base matrix changes according to the code rate. The QC-dual-diagonal matrix in (5) has the parity structure of a QC-irregular repeat-accumulate (QC-IRA) code, which can be implemented by a single accumulator [12].

2.2 | Dominant FASs

For an (N, K) LDPC code, the parity-check matrix $\mathbf{H}$ can be depicted as a Tanner graph G whose nodes are a union of check nodes $C = \{c_j | j = 1, 2, \dots, M\}$ and variable nodes $V = \{v_i | i = 1, 2, \dots, N\}$. The edge between a check node c_j and variable node v_i is connected if $h_{ji} = 1$. For any subset $\mathcal{S} \subseteq V$, a subgraph $G_{\mathcal{S}}$ that consists of variable nodes $v_i \in \mathcal{S}$ and check nodes adjacent to v_i can be induced. Let $O_{\mathcal{S}}$ and $E_{\mathcal{S}}$ be a set of check nodes with odd-degree and even-degree in $G_{\mathcal{S}}$, respectively.

> **Definition 1.** A subset $\mathcal{S} \subseteq V$ is (a,b) TS if $a = |\mathcal{S}|$ and $b = |O_{\mathcal{S}}|$.

> **Definition 2.** A subset $\mathcal{S} \subseteq V$ is elementary if every $c_j \in G_{\mathcal{S}}$ has a degree of one or two.

> **Definition 3.** A subset $\mathcal{S} \subseteq V$ is (a,b) AS if $\mathcal{S}$ is (a,b) TS, and every $v_i \in \mathcal{S}$ is connected to more $c_j \in E_{\mathcal{S}}$ than $c_{j'} \in O_{\mathcal{S}}$.

> **Definition 4.** A subset $\mathcal{S} \subseteq V$ is (a, b) FAS if $\mathcal{S}$ is (a, b) AS, and every $v_i \in V \setminus S$ is connected to more $c_j \in C \setminus O_{\mathcal{S}}$ than $c_{j'} \in O_{\mathcal{S}}$.

In general, the dominant TS $\mathcal{S}$ comprises short cycles inherent in G, breaking the independence of the extrinsic information for subsequent iterations. The check nodes in $E_{\mathcal{S}}$ connected to an even number of variable nodes of $\mathcal{S}$ are falsely satisfied. Although the check nodes in $O_{\mathcal{S}}$ are capable of correcting wrong information, b check nodes are not sufficient to correct them. Among these TSs, small elementary FASs have the most dominant effects on the error floor.

2.3 | Importance sampling

The block error rate (BLER) of an LDPC code in the high signal-to-noise ratio (SNR) regime can be estimated by the mean translation-based importance sampling method. Let us assume that an all-zeros codeword $\mathbf{x} = \mathbf{0}_N$ with binary phase-shift keying symbol $\mathbf{s} = \mathbf{1}_N$ is transmitted because of the symmetricity of the LDPC code. In the binary-input additive white Gaussian noise channel, the received symbol is denoted by $\mathbf{r} = \mathbf{s} + \mathbf{z}$ where $\mathbf{z} \sim N(\mathbf{0}_N, \sigma^2 \mathbf{I}_{N \times N})$. The importance sampling estimator for TS $\mathcal{S}$ can be formulated as

$$\hat{P}_{\mathcal{S}} = \frac{1}{L_{\mathcal{S}}} \sum_{l=1}^{L_{\mathcal{S}}} I_E(\mathbf{r}_l) w(\mathbf{r}_l), \tag{6}$$

where $L_{\mathcal{S}}$ is the number of trials; $I_E(\mathbf{r})$ is the indicator function of error event E; and $w(\mathbf{r})$ is the weight function given as

$$w(\mathbf{r}) = \exp\left(\frac{-\|\mathbf{r} - \mathbf{1}_N\|^2 + \|\mathbf{r} - \mathbf{1}_N + \boldsymbol{\mu}\|^2}{2\sigma^2} \right), \tag{7}$$

where $\boldsymbol{\mu}$ is a mean bias with $\mu_i = \|\mathbf{e}_S\|/\sqrt{|S|}$ for $v_i \in S$ and $\mu_i = 0$ otherwise, and $\mathbf{e}_S$ is an error vector toward the error boundary for S [17]. The confidence interval of $\hat{P}_S$ can be calculated by a variance estimator defined as

$$\widehat{\text{var}}[\hat{P}_S] = \frac{1}{L_S} \sum_{l=1}^{L_S} \frac{1}{L_S} \left\{ I_E(\mathbf{r}_l) w(\mathbf{r}_l) - \hat{P}_S \right\}^2. \tag{8}$$

To achieve a confidence level identical to that achieved with a Monte Carlo simulation for which N_{err} error events are observed, the normalized error ϵ of $\hat{P}_S$ is such that [22]

$$\epsilon = \frac{\sqrt{\widehat{\text{var}}[\hat{P}_S]}}{\hat{P}_S} \leq \frac{1}{\sqrt{N_{\text{err}}}}. \tag{9}$$

3 | DOMINANT FAS SEARCH METHOD

The Tanner graph of a Raptor-like LDPC code has various types of TSs because it comprises cycles of various lengths and degree-1 variable nodes. Because of these structural properties, the existing TS search methods are ineffective when applied for the code. Although the algorithm in Karimi and Banihashemi [16] guarantees finding all small TSs for regular LDPC codes, relatively large TSs may not be searched for irregular LDPC codes. The AS search method for 5G NR LDPC codes proposed in Otarinia [18] cannot find the most dominant (34, 1) or (53, 0) FASs of 5G NR BG2 (1664, 320) LDPC code owing to computational complexity. In this paper, an effective method is proposed to identify dominant FASs for Raptor-like LDPC codes.

Let define C_1 as

$$C_1 \triangleq \{c_j | M_1 < j \leq M\}, \tag{10}$$

which is a subset of C corresponding to the rows of submatrix $[\mathbf{H}_{\text{IRC}} \ \mathbf{I}]$. Each check node in C_1 is adjacent to a degree-1 variable node. For a Raptor-like LDPC code, let us define a subset $S \subseteq V$ as (a, b, c) TS if S is (a, b) TS, and $c = |O_S \cap C_1^c|$. According to the definition of FAS, it can be easily shown that for FAS S, if there exists a check node $c_j \in O_S$, then $c_j \notin C_1$. Thus, for an (a, b, c) FAS, c is equal to b. As an FAS with small b has a dominant effect on the error floor, (a, b, c) TS with a small c is likely to be a subset of the dominant FAS.

In general, the dominant TSs consist of unions of short cycles inherent in Tanner graphs. The proposed FAS search method first overlaps short cycles to be expanded into elementary TSs. The degrees of variable nodes in $\mathbf{H}_{\text{HRC}}$ are two, three, or four for 5G NR BG1 LDPC codes, two or three for 5G NR BG2 LDPC codes, and two or three for ATSC 3.0 type A LDPC codes. For an elementary (a, b, c) TS S, if there exists a variable node $v_i \notin S$

adjacent to two check nodes $c_{j_1}, c_{j_2} \in O_S$, and S can be expanded into elementary (a', b', c') TS $S' = S \cup \{v_i\}$. All possible cases of extension to S' are as follows:

i. If $c_{j_1}, c_{j_2} \in C_1$, then $a' = a+1$, $b' \geq b$, and $c' \geq c+2$, as there exist at least two check nodes adjacent to v_i that are included in $O_{S'} \cap C_1^c$.

ii. If $c_{j_1} \in C_1$ and $c_{j_2} \notin C_1$, then $a' = a+1$, $b' \geq b-1$, and $c' \geq c$, as $c_{j_2} \in E_{S'} \cap C_1^c$, and there exists at least one check node adjacent to v_i that is included in $O_{S'} \cap C_1^c$.

iii. If $c_{j_1}, c_{j_2} \notin C_1$, then $a' = a+1$, $b' \geq b-2$, and $c' \geq c-2$, as $c_{j_1}, c_{j_2} \in E_{S'} \cap C_1^c$.

Algorithm 1 Dominant FAS search method for Raptor-like LDPC codes

---

Input: Tanner graph G with girth g, $G_{\text{HRC}}, L, T,$ and J
Output: $\mathcal{L}_{\text{FAS},i}$ for $i = 1, \cdots, (L - g/2 + 1)$.
$\mathcal{L}_{\text{TS},0} \leftarrow \emptyset$. Find the short cycles in G and list them in $\mathcal{L}_{\text{cycle}}$.
for $S \in \mathcal{L}_{\text{cycle}}$ **do**
    Calculate a, b, and c of S.
    if $(a + b \leq T)$ and $(c \leq J)$ **then**
        $\mathcal{L}_{\text{TS},0} \leftarrow \mathcal{L}_{\text{TS},0} \cup \{S\}$.
    end if
end for
for $i = 1, \cdots, (L - g/2 + 1)$ **do**
    $\mathcal{L}_{\text{TS},i} \leftarrow \emptyset$.
    for $S \in \mathcal{L}_{\text{TS},i-1}$ **do**
    Find all the paths of the shortest length connecting two check nodes in $O_S \cap C_1^c$ in G_{HRC}. Let V_S be a set of variable nodes of the shortest paths. $\mathcal{L}_S = \cup \{V_S\}$.
        for $V_S \in \mathcal{L}_S$ **do**
            $S' \leftarrow S \cup V_S$ and calculate a, b, and c of S'.
            if $(S' \notin \mathcal{L}_{\text{TS},i})$ and $(a + b \leq T)$ and $(c \leq J)$ **then**
                $\mathcal{L}_{\text{TS},i} \leftarrow \mathcal{L}_{\text{TS},i} \cup \{S'\}$.
            end if
        end for
    end for
end for
for $i = 1, \cdots, (L - g/2 + 1)$ **do**
    $\mathcal{L}_{\text{FAS},i} \leftarrow \emptyset$.
    for $S \in \mathcal{L}_{\text{TS},i}$ **do**
        for $c_j \in O_S \cap C_1$ **do**
            Find degree-1 variable node v_i adjacent to c_j.
            $S \leftarrow S \cup v_i$.
        end for
    end for
    if S is FAS **then**
        $\mathcal{L}_{\text{FAS},i} \leftarrow \mathcal{L}_{\text{FAS},i} \cup \{S\}$.
    end if
end for

From the above discussion, c decreases only in Case iii. For an elementary (a, b, c) TS $\mathcal{S}$, suppose that there exists a variable node $v_{i_1} \notin \mathcal{S}$ adjacent to a check node $c_{j_1} \in O_{\mathcal{S}}$ and another variable node $v_{i_2} \notin \mathcal{S}$ adjacent to a check node $c_{j_2} \in O_{\mathcal{S}}$ and that v_{i_1} and v_{i_2} are connected by c_{j_3}. Then, $\mathcal{S}$ can be expanded into elementary (a', b', c') TS $\mathcal{S}' = \mathcal{S} \cup \{v_{i_1}, v_{i_2}\}$ with all possible cases of extension as follows:

i. If $c_{j_1}, c_{j_2}, c_{j_3} \in C_1$, then $a' = a + 2$, $b' \geq b + 2$, and $c' \geq c + 4$, as there exist at least two check nodes adjacent to each v_{i_1} and v_{i_2}, which are included in $O_{\mathcal{S}'} \cap C_1^c$.

ii. If $c_{j_1}, c_{j_2} \in C_1$ and $c_{j_3} \notin C_1$, then $a' = a + 2$, $b' \geq b$, and $c' \geq c + 2$, as there exists at least one check node adjacent to each v_{i_1} and v_{i_2}, which is included in $O_{\mathcal{S}'} \cap C_1^c$.

iii. If $c_{j_1}, c_{j_3} \in C_1$ and $c_{j_2} \notin C_1$, then $a' = a + 2$, $b' \geq b + 1$, and $c' \geq c + 2$, as $c_{j_2} \in E_{\mathcal{S}'} \cap C_1^c$, and there exist at least two check nodes adjacent to v_{i1}, and there exists at least one check node adjacent to v_{i_2}, such that all of these check nodes are included in $O_{\mathcal{S}'} \cap C_1^c$.

iv. If $c_{j_1} \in C_1$ and $c_{j_2}, c_{j_3} \notin C_1$, then $a' = a + 2$, $b' \geq b - 1$, and $c' \geq c$, as $c_{j_2}, c_{j_3} \in E_{\mathcal{S}'} \cap C_1^c$, and there exists at least one check node adjacent to v_{i_1}, which is included in $O_{\mathcal{S}'} \cap C_1^c$.

v. If $c_{j_1}, c_{j_2} \notin C_1$ and $c_{j_3} \in C_1$, then $a' = a + 2$, $b' \geq b$, and $c' \geq c$, as $c_{j_1}, c_{j_2} \in E_{\mathcal{S}'} \cap C_1^c$, and there exists at least one check node adjacent to each v_{i_1} and v_{i_2}, which is included in $O_{\mathcal{S}'} \cap C_1^c$.

vi. If $c_{j_1}, c_{j_2}, c_{j_3} \notin C_1$, then $a' = a + 2$, $b' \geq b - 2$, and $c' \geq c - 2$, as $c_{j_1}, c_{j_2}, c_{j_3} \in E_{\mathcal{S}'} \cap C_1^c$.

From the above discussion, c decreases only in Case vi. The same discussion can be developed for the situation of appending more than two variable nodes into an elementary TS. Hence, appending variable nodes adjacent to unsatisfied check nodes not included in C_1 is an effective method to search for the elementary TSs that are subsets of dominant FASs. Hence, the searching procedure is decoupled into two steps. First, the elementary TSs are expanded into larger elementary TSs inside a subgraph G_{HRC} corresponding to $\mathbf{H}_{\text{HRC}}$. Next, for an elementary TS to be expanded into the elementary FAS, the degree-1 variable nodes adjacent to the unsatisfied check nodes in C_1 are appended to it. The pseudocode of the dominant FAS search method is presented in Algorithm 1.

As a search space is reduced to a subgraph G_{HRC} instead of the whole Tanner graph G, the time-efficiency of the algorithm is greatly improved compared to the algorithm that searches the entire G. In addition, the effectiveness of identifying relatively large dominant FASs is also enhanced because reducing the search space solves the suboptimality that relatively large TSs may not

be found by the iterative cycle-overlapping procedure for irregular LDPC codes.

In the cycle-overlapping procedure, the maximum value of c is set as J to reduce computational complexity. The maximum value of $(a + b)$ of TS is set as T. This restriction reduces the computational complexity because only small dominant sets are searched. Under this restriction, the proposed method can find the same FASs as an unrestricted method based on the assumption that variable nodes have degrees larger than two. The value of $(a + b)$ does not decrease in the iterative cycle-overlapping procedure under the said assumption.

4 | NUMERICAL RESULTS

4.1 | FAS enumerators of Raptor-like LDPC codes

The proposed method is employed to identify the dominant FASs of 5G NR BG2 LDPC codes with short blocklengths and those of 5G NR BG1 LDPC code and ATSC 3.0 type A LDPC code with large blocklengths. The method is implemented in Python. The execution time described herein corresponds to a desktop computer with 3.6 GHz CPU and 32 GB RAM.

Table 1 lists the (a, b) FASs of 5G NR BG2 $(1664, 320)$ LDPC code with lifting size $Z = 32$ enumerated by the proposed FAS search algorithm, and the whole graph search (WGS) algorithm containing the cycle overlapping procedure that is reported in Karimi and Banihashemi [16]. The FASs with $b = 0$ are the low-weight codewords [17]. FASs with $a \leq 41$ and $0 < b \leq 2$ ($a \leq 60$ for $b = 0$) are listed as small TSs with $a \leq \sqrt{N}$ exhibit dominant effects on the error floor [15]. The girth g of the code is four, and the cycles of length shorter than eight are found in the search methods. Parameter L is set as 10, and T is set as 60 for both methods. Four smallest values of c are found for each a in the proposed method, while 12 smallest values of c are found with the WGS algorithm. The execution time for the proposed algorithm is about 56 min, which is one seventh that of the WGS algorithm. Meanwhile, relatively large FASs such as $(50, 0)$, $(53, 0)$, and $(41, 1)$ FASs are only found by the proposed algorithm. These sets are frequently observed in the high SNR regime in the Monte Carlo simulation. The method proposed in Otarinia [18] cannot find the most dominant $(25, 2)$ and $(34, 1)$ FASs because of computational complexity.

The topologies of $(34, 1)$ and $(53, 0)$ FASs of 5G NR BG2 $(1664, 320)$ LDPC code, respectively, are shown in Figure 2. The index i of each variable node v_i is shown to the left of the variable node. Even-degree check nodes in

TABLE 1 Fully absorbing set (FAS) enumerators of 5G NR BG2 (1664, 320) low-density parity-check (LDPC) code and the execution time of FAS search methods

(*a*, *b*) FAS	Proposed Count	WGS algorithm
(50, 0)	32	–
(53, 0)	32	–
(58, 0)	32	–
(59, 0)	32	–
(34, 1)	32	32
(41, 1)	64	32
(19, 2)	32	32
(24, 2)	48	48
(25, 2)	32	32
(26, 2)	32	32
(27, 2)	64	64
(28, 2)	64	64
(29, 2)	64	64
(30, 2)	64	64
(31, 2)	32	32
(32, 2)	192	160
(33, 2)	96	64
(34, 2)	128	64
(35, 2)	160	64
(36, 2)	160	96
(37, 2)	32	–
(38, 2)	288	96
(39, 2)	288	64
(40, 2)	352	64
(41, 2)	256	–
Execution time (min)	56	389

TABLE 2 FAS enumerators of 5G NR BG2 (3328, 640) LDPC code and execution time of the FAS search methods

(*a*, *b*) FAS	Proposed Count	WGS algorithm
(60, 0)	64	–
(72, 0)	64	–
(78, 0)	64	–
(41, 1)	64	64
(43, 1)	64	–
(44, 1)	64	64
(46, 1)	64	64
(50, 1)	64	–
(55, 1)	64	–
(56, 1)	192	–
(24, 2)	64	64
(30, 2)	64	64
(32, 2)	192	192
(34, 2)	64	64
(37, 2)	64	64
(38, 2)	192	128
(39, 2)	64	–
(41, 2)	128	64
(42, 2)	128	128
(43, 2)	64	–
(44, 2)	128	64
(45, 2)	64	–
(46, 2)	128	128
(47, 2)	320	128
(48, 2)	192	–
(49, 2)	128	–
(50, 2)	192	128
(51, 2)	192	64
(52, 2)	256	–
(53, 2)	128	–
(54, 2)	384	–
(55, 2)	448	–
(56, 2)	512	–
(57, 2)	576	–
(58, 2)	704	–
Execution time (min)	119	1103

Abbreviation: FAS, fully absorbing set.

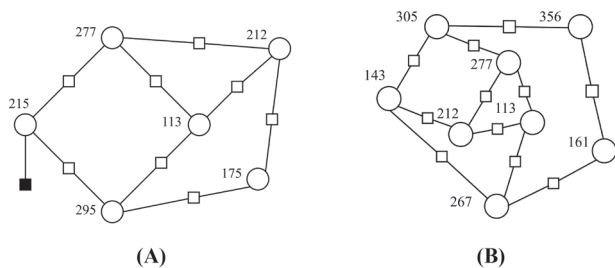**FIGURE 2** Topologies of the dominant fully absorbing sets (FASs) of 5G NR BG2 (1664, 320) LDPC code (○ = variable nodes, □ = even-degree check nodes, ■ = odd-degree check nodes): (A) (34, 1) FAS and (B) (53, 0) FAS

C_1 and their adjacent degree-1 variable nodes are omitted for simplicity. These FASs are the most frequently observed ones in the Monte Carlo simulation, implying that they have the most dominant effects on the error floor of the code. As can be seen from Figure 2, the dominant sets of 5G NR LDPC codes are unions of cycles with various lengths. The even-degree check nodes shown in Figure 2 are not in C_1 for both sets, as elaborated in Section 3.

The proposed method has the advantage of finding for relatively large FASs. For instance, in the iterative cycle-overlapping procedure of the proposed method, $\mathcal{S} = \{143, 212, 277, 305\}$ is expanded to $\mathcal{S} \to \mathcal{S} \cup \{113\} \to \mathcal{S} \cup \{113, 267\} \to \mathcal{S} \cup \{113, 161, 267, 356\}$, where the last set is a subset of $(53, 0)$ FAS shown in Figure 2B. In contrast, the cycle-overlapping procedure in the WGS algorithm expands S into $\mathcal{S} \to \mathcal{S} \cup \{113\} \to \mathcal{S} \cup \{113, 267\} \to \mathcal{S} \cup \{13, 113, 267\}$, where the last set is the subset of $(41, 5)$ FAS that does not adversely affect the error floor of the code. The proposed method is effective for Raptor-like LDPC codes as it reduces the search space into subgraph G_{HRC} where the most subsets of the dominant FASs exist.

Table 2 lists the FASs with $a \leq 58$ and $0 < b \leq 2$ ($a \leq 80$ for $b = 0$) of 5G NR BG2 $(3328, 640)$ LDPC code with a lifting size $Z = 64$ as found by the proposed method and the WGS algorithm, respectively. Here, the girth g of the code is six, and all the parameters are the same as in the previous description, except that $T = 80$. The time required by the proposed algorithm for the code is twice that for the 5G NR BG2 $(1664, 320)$ LDPC code, which is linearly proportional to the blocklength. For a larger blocklength K, the relative search-effectiveness of the proposed algorithm is higher than that of the WGS algorithm owing to the reduction in the search space.

Figure 3 shows the BLER performances of 5G NR BG2 LDPC codes with the Monte Carlo simulation (solid line) and importance sampling simulation (dotted line). The BLER performances of the codes with blocklength $K = 320$ and $K = 640$ are presented in Figure 3A,B, respectively. The row-layered sum-product algorithm (SPA) decoder [13] with a maximum iteration number of 20 is used for both simulations. The code rates range from 1/4 to 10/13, where the two leftmost columns of the base matrices are punctured [5]. In the Monte Carlo simulation, 50 decoding errors were collected. The importance sampling simulation was terminated when ϵ became less than $1/\sqrt{20}$; further, in this simulation, BLER is estimated as a sum of $\widehat{P}_{\mathcal{S}}$ for all $\mathcal{S}$ identified by the proposed FAS search method, as listed in Tables 3 and 4 for $K = 320$ and $K = 640$, respectively. The cumulative $\widehat{P}_{\mathcal{S}}$ of the automorphic sets are calculated as the product of the estimator of a set randomly chosen from them and the number of the automorphic sets, assuming the automorphic sets in a QC-LDPC code have equivalent $\widehat{P}_{\mathcal{S}}$.[1] As shown in Figure 3, the BLER estimation with the importance sampling method closely matches the

---

[1] Note that the number of the automorphic TSs is mostly Z with a few exceptions; for example, there are $Z/2 = 16$ automorphic $(24, 2)$ FASs for 5G NR BG2 $(1664, 320)$ LDPC code as shown in Table 1.
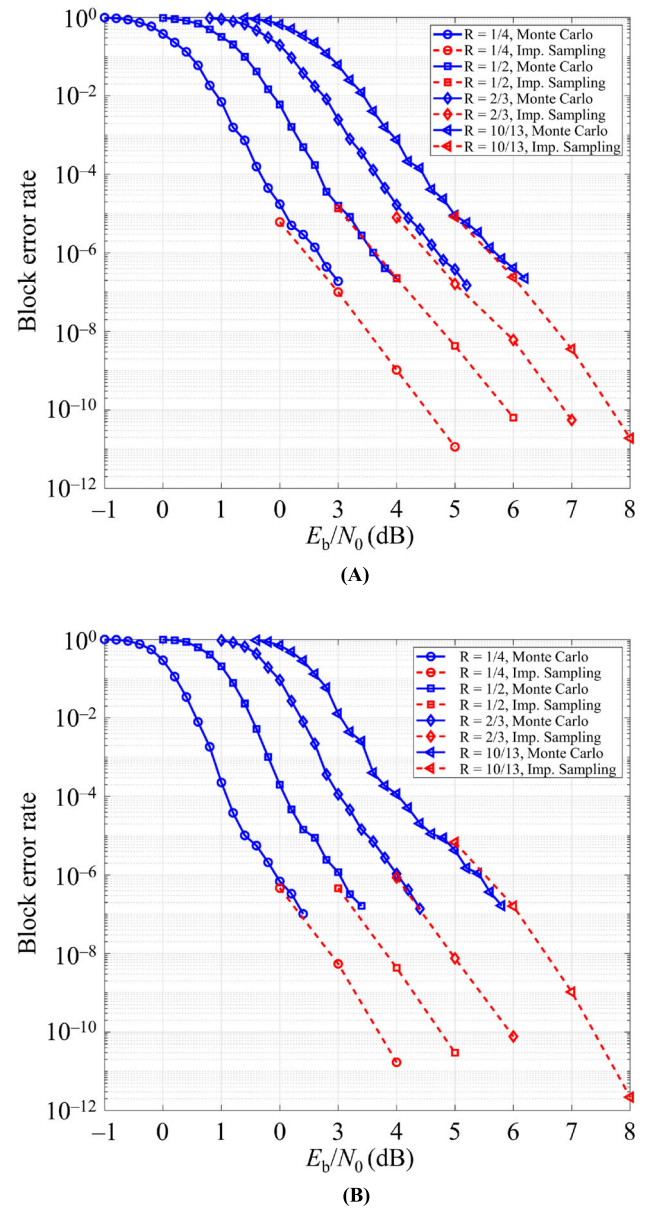

(A)

(B)

FIGURE 3 Monte Carlo and importance sampling block error rate (BLER) estimation of 5G NR BG2 LDPC codes for different blocklengths and code rates: (A) Block length $K = 320$ and (B) block length $K = 640$

estimation by the Monte Carlo simulation. The results imply that the proposed method can identify the most dominant FASs of 5G NR LDPC codes regardless of the lifting size Z, blocklength K, code rate R, or girth g of the Tanner graph G.

Table 5 lists the FASs with $a \leq 48$ and $0 < b \leq 2$ of 5G NR BG1 $(11968, 3872)$ LDPC code with a lifting size $Z = 176$ as obtained by the proposed method. Parameter L is set as 10, and T is set as 50. The four smallest values of c are found for each a. The girth g of the code is 4, and cycles of length shorter than 8 are found. The

TABLE 3 Dominant FAS enumerator of 5G NR BG2 LDPC code with a blocklength $K = 320$

Code rate R	(a, b) FAS	Base matrix column index in H_{HRC}
$R = 1/4$	$(41, 0)$	4, 5, 7, 8, 8, 9, 14
	$(30, 1)$	4, 6, 7, 7, 9, 10
	$(24, 2)$	4, 5, 7, 8, 9
$R = 1/2$	$(12, 1)$	4, 6, 7, 7, 9, 10
	$(13, 1)$	3, 4, 4, 7, 9, 9, 13, 13
	$(10, 2)$	4, 6, 7, 9, 10
$R = 2/3$	$(11, 0)_1$	2, 3, 10, 12, 14
	$(11, 0)_2$	2, 5, 6, 9, 10, 10, 11, 13, 14
	$(7, 1)$	4, 6, 7, 7, 9, 10
$R = 10/13$	$(7, 0)_1$	2, 3, 10, 12, 14
	$(7, 0)_2$	1, 6, 6, 8, 10, 13

Abbreviation: FAS, fully absorbing set.

TABLE 4 Dominant FAS enumerator of 5G NR BG2 LDPC code with a blocklength $K = 640$

Code rate R	(a, b) FAS	Base matrix column index in H_{HRC}
$R = 1/4$	$(44, 0)$	3, 6, 7, 9, 10, 11, 13, 13
	$(34, 1)_1$	4, 5, 8, 10, 13, 14
	$(34, 1)_2$	3, 4, 5, 9, 13, 13, 14
	$(38, 1)$	3, 4, 8, 9, 10, 13, 13
$R = 1/2$	$(18, 0)$	3, 6, 7, 9, 10, 11, 13, 13
	$(12, 1)$	3, 4, 5, 9, 13, 13, 14
$R = 2/3$	$(11, 0)$	3, 6, 7, 9, 10, 11, 13, 13
	$(7, 1)$	3, 4, 5, 9, 13, 13, 14
	$(9, 1)$	2, 3, 4, 9, 13, 14
$R = 10/13$	$(7, 0)$	1, 6, 6, 8, 10, 13
	$(5, 2)_1$	1, 6, 8, 10
	$(5, 2)_2$	1, 6, 10, 13

Abbreviation: FAS, fully absorbing set.

TABLE 5 FAS enumerator of 5G NR BG1 (11968,3872) LDPC code

(a, b) FAS	Count	(a, b) FAS	Count
$(24, 1)$	176	$(32, 2)$	352
$(41, 1)$	176	$(33, 2)$	528
$(43, 1)$	176	$(34, 2)$	880
$(45, 1)$	352	$(35, 2)$	352
$(46, 1)$	528	$(36, 2)$	1056
$(47, 1)$	176	$(37, 2)$	1760
$(11, 2)$	176	$(38, 2)$	704
$(16, 2)$	176	$(39, 2)$	1232
$(18, 2)$	88	$(40, 2)$	2288
$(20, 2)$	176	$(41, 2)$	352
$(21, 2)$	176	$(42, 2)$	528
$(23, 2)$	352	$(43, 2)$	1584
$(24, 2)$	176	$(44, 2)$	1408
$(27, 2)$	352	$(45, 2)$	1760
$(28, 2)$	176	$(46, 2)$	2288
$(29, 2)$	704	$(47, 2)$	5280
$(30, 2)$	176	$(48, 2)$	2640

Abbreviation: FAS, fully absorbing set.

TABLE 6 FAS enumerator of ATSC 3.0 type A (16200,2160) LDPC code

(a, b) FAS	Count	(a, b) FAS	Count
$(33, 3)$	360	$(58, 4)$	3960
$(40, 3)$	1800	$(60, 4)$	720
$(65, 3)$	1080	$(63, 4)$	1080
$(33, 4)$	1080	$(65, 4)$	2880
$(38, 4)$	720	$(66, 4)$	360
$(40, 4)$	4680	$(68, 4)$	720
$(48, 4)$	360	$(70, 4)$	3600
$(53, 4)$	1440		

Abbreviation: FAS, fully absorbing set.

computational complexity of the search method for large blocklengths mainly depends on the girth and the configuration of the short cycles in the Tanner graph. The required time for the search method is about 4 days, and most of this time is spent for the cycle-overlapping procedure, as the code contains cycles of various lengths. Unlike the 5G NR BG2 LDPC codes, using the proposed method, many small FASs can be observed in the code despite the large K and N.

Table 6 lists the FASs with $a \leq 70$ and $0 < b \leq 4$ of ATSC 3.0 type A $(16200, 2160)$ LDPC code with a lifting size $Z = 360$ as found by the proposed method. Parameter L is set as 14, and T is set as 130. The four smallest values of c are found for each a. The girth g of the code is 12, and cycles of length shorter than 16 are found. The required time for the search method is about 4 days, and most of this time is spent searching for the cycles because of the large girth. ATSC 3.0 type A LDPC codes allow multiple edges and have large girths to provide very low BLER for very long code lengths and limited number of code rates [6]. Therefore, neither low-weight codewords nor small FAS with the b value <3 are observable in the ATSC 3.0 type A $(16200, 2160)$ LDPC code.

4.2 | Discussion on 5G NR rate-matching for short blocklengths

In 5G NR LDPC codes, the rate-matching schemes, that is, shortening and puncturing, lower the error rate for short blocklengths. At the transmitter, the shortened bits are filled with zeros and then encoded into a codeword, and both the shortened and punctured bits are not transmitted. At the receiver, the reliability of the shortened and punctured bits are filled with the maximum values and zeros, respectively. Specifically, the lifting size Z and parameter K_b are selected according to the data length B. Parameter K_b determines how many rightmost columns among the columns of the base matrix corresponding to the information bits are to be shortened. For example, K_b is selected as 8 for $192 < B \le 560$ in BG2, implying that the 9th and 10th columns are shortened [5]. On the other hand, the leftmost two columns of the base matrix are always punctured as puncturing the variable nodes with high degrees reduces the thresholds [3–5].

If the variable nodes in an FAS are shortened, the effect of the FAS on the error floor is weakened [18,23]. Figure 4 shows the BLER performances of 5G NR BG2 LDPC code with a blocklength $K = 320$ and a code rate $R = 256/576$ corresponding to various shortening patterns. The error floors of the shortened codes depend on the shortening patterns. For the 8th and 10th column shortening pattern, (13, 1) FASs in Table 3 have dominant effects on the error floor, resulting in higher error floors. On the other hand, for the 7th and 9th column

shortening pattern or for the 9th and 10th column shortening pattern of 5G NR standard, the error floors are lower. For the 7th and 8th column shortening pattern, the dominant FASs listed in Table 3 are weakened, resulting in a lower error floor compared with that of the 8th and 10th column shortening pattern. However, the shortened code still has a high error floor, implying that the FAS configuration after shortening should be considered to effectively reduce the error floor.

As shown in Tables 3 and 4, the leftmost two punctured columns, namely, the first and second columns in the base matrices, cannot form the most dominant FASs at low code rates because these variable nodes are designed to have high degrees. Therefore, the punctured variable nodes can be successfully recovered in the decoding process, while reducing the thresholds remarkably. However, as the code rate increases, the degrees of the punctured variable nodes also decrease, and thus, they also exist in the dominant FASs. For high code rates, puncturing of the leftmost two columns does not guarantee the recovery of the punctured nodes at a high SNR.

5 | CONCLUSION

In this paper, an effective method to identify the dominant FASs of Raptor-like LDPC codes by optimizing the search space in their Tanner graphs is proposed. This method enumerates the most dominant FASs of 5G NR LDPC codes and ATSC 3.0 type A LDPC code in the simulation results. The results prove that the proposed method finds more dominant FASs within a shorter execution time than that possible with the existing search algorithm. In particular, relatively large dominant FASs are only identified by the proposed method. From the perspective of the observed FAS enumerators, the paper discusses how the 5G NR rate-matching design affects the decoder for short blocklengths. Density evolution alone cannot guarantee the best error-rate performance in a short blocklength regime. Hence, the proposed FAS search method can be expected to play a role in designing low-floor Raptor-like LDPC codes or decoders for URLLC applications.
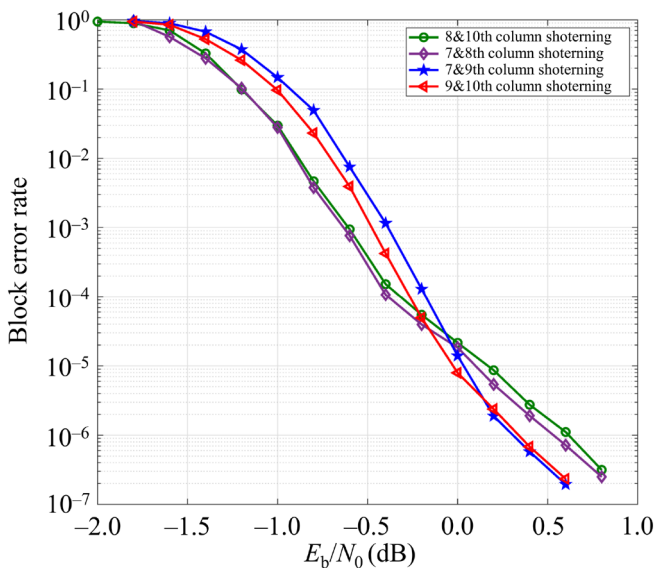

FIGURE 4 Block error rate (BLER) performances of 5G New Radio (NR) base graph (BG) 2 low-density parity-check (LDPC) code with a code rate $R = 256/576$ for different shortening patterns

ORCID

Woncheol Cho https://orcid.org/0000-0001-7787-1101

REFERENCES

1. M. Sybis, K. Wesolowski, K. Jayasinghe, V. Venkatasubramanian, and V. Vukadinovic, *Channel coding for ultra-reliable low-latency communication in 5G systems*, (IEEE 84th Vehicular Technology Conference, Montreal, Canada), 2016. https://doi.org/10.1109/VTCFall.2016.7880930

2. M. C. Coşkun, G. Durisi, T. Jerkovits, G. Liva, W. Ryan, B. Stein, and F. Steiner, *Efficient error-correcting codes in the short blocklength regime*, Phys. Commun. **34** (2019), 66–79.

3. T. Chen, K. Vakilinia, D. Divsalar, and R. D. Wesel, *Protograph-based Raptor-like LDPC codes*, IEEE Trans. Commun. **63** (2015), no. 5, 1522–1532.

4. T. Chen, D. Divsalar, J. Wang, and R. D. Wesel, *Protograph-based Raptor-like LDPC codes for rate compatibility with short blocklengths*, (IEEE Global Telecommunications Conference - GLOBECOM 2011, Houston,TX, USA), 2011. https://doi.org/10.1109/GLOCOM.2011.6134051

5. *NR; Multiplexing and channel coding*, version 1.0.1, Release 15, 3GPP Standard TS 38.212, 2017.

6. K.-J. Kim, S. Myung, S.-I. Park, J.-Y. Lee, M. Kan, Y. Shinohara, J.-W. Shin, and J. Kim, *Low-density parity-check codes for ATSC 3.0*, IEEE Trans. Broadcast. **62** (2016), no. 1, 189–196.

7. *ATSC Standard Physical Layer Protocol Document A/322*, Adv. Telev. Syst. Committee, Washington, DC, USA, 2021.

8. T. J. Richardson and R. L. Urbanke, *Efficient encoding of low-density parity-check codes*, IEEE Trans. Inf. Theory **47** (2001), no. 2, 638–656.

9. T. Nguyen, T. Nguyen Tan, and H. Lee, *Efficient QC-LDPC encoder for 5G New Radio*, Electron. **8** (2019), no. 6, 1–15.

10. J. H. Bae, A. Abotabl, H.-P. Lin, K.-B. Song, and J. Lee, *An overview of channel coding for 5G NR cellular communications*, APSIPA Trans. Signal Inf Process. **8** (2019), 1–14.

11. T. Richardson and S. Kudekar, *Design of low-density parity check codes for 5G New Radio*, IEEE Commun. Mag. **56** (2018), no. 3, 28–34.

12. W. Ryan and S. Lin, *Channel codes: Classical and modern*, Cambridge University Press, 2009.

13. D. E. Hocevar, *A reduced complexity decoder architecture via layered decoding of LDPC codes*, (IEEE Workshop onSignal Processing Systems, Austin, TX, USA), 2004, pp. 107–112.

14. Samsung, *Design of short-length LDPC codes*, 3GPP TSG RAN WG1, Tdoc R1-1609069, Meeting #86bis, 2016.

15. S. Landner and O. Milenkovic, *Algorithmic and combinatorial analysis of trapping sets in structured LDPC codes*, (International Conference on Wireless Networks, Communications and Mobile Computing, Maui, HI, USA), 2005, pp. 630–635.

16. M. Karimi and A. H. Banihashemi, *Efficient algorithm for finding dominant trapping sets of LDPC codes*, IEEE Trans. Inf. Theory **58** (2012), no. 1, 6942–6958.

17. C. A. Cole, S. G. Wilson, E. Hall, and T. R. Giallorenzi, *A general method for finding low error rates of LDPC codes*, arXiv preprint, 2006, pp. 1–30. https://doi.org/10.48550/arXiv.cs/0605051

18. M. Otarinia, *Absorbing sets and error floor performance of the 5G New Radio code*, University of Notre Dame, 2019.

19. Y. Hashemi and A. H. Banihashemi, *Characterization of elementary trapping sets in irregular LDPC codes and the corresponding efficient exhaustive search algorithms*, IEEE Trans. Inf. Theory **64** (2018), no. 5, 3411–3430.

20. IEEE Standard for Information Technology-Local and Metropolitan Area Networks-Specific Requirements-Part 11 Wireless LAN medium access control (MAC) and physical layer (PHY) specifications amendment 5: Enhancements for higher throughput, 2009, IEEE Standard 802.11n-2009.

21. IEEE Standard for Local and Metropolitan Area Networks-Part 16, Air interface for fixed and mobile broadband wireless access systems amendment 2: Physical and medium access control layers for combined fixed and mobile operation in licensed bands and corrigendum 1, 2006, IEEE Standard 802.16e-2005 and 802.16-2004/Cor 1–2005.

22. E. Cavus, C. L. Haymes, and B. Daneshrad, *An IS simulation technique for very low BER performance evaluation of LDPC codes*, (IEEE International Conference on Communications, Istanbul, Turkey), 2006. https://doi.org/10.1109/ICC.2006.254893

23. S.-R. Kim and D.-J. Shin, *Lowering error floors of systematic LDPC codes using data shortening*, IEEE Commun. Lett. **17** (2013), no. 12, 2348–2351.

AUTHOR BIOGRAPHIES

Woncheol Cho received the BS and MS degrees in Information and Communications Engineering from Daegu Gyeongbuk Institute of Science and Technology, Daegu, Republic of Korea, in 2018 and 2020, respectively. He is currently a researcher with Electronics and Telecommunications Research Institute, Daejeon, Republic of Korea. His research interests include wireless network design and channel coding.

Chanho Yoon received the BS degree from Korea University, Seoul, Republic of Korea in 2003, and MS and PhD degrees both in Electrical Engineering from Korea Advanced Institute of Science and Technology, Daejeon, Republic of Korea, respectively, in 2005 and 2011. He has worked for Electronics and Telecommunications Research Institute as a principal engineer since 2005. His research interests include multi-antenna joint transmission combined with error-control coding techniques and their application in ultra-reliable communications and communication systems engineering.

Kapseok Chang received the PhD degree in Information and Communications Engineering from the Korea Advanced Institute of Science and Technology, Daejeon, Republic of Korea, in 2005, respectively. Since July 2005, he has been with Electronics and Telecommunications Research Institute (ETRI), Daejeon, Republic of Korea as a full-time senior researcher. Since September 2009, he has also been an associate professor of Mobile Communication and Digital Broadcasting Engineering with University of Science and Technology, Republic of Korea. From March 2011 to February 2013, he was with the School of Engineering Science, Simon Fraser University, Burnaby, Canada, as a visiting professor. His research interests include smart antennas, OFDM, synchronization, interference cancelation, in-band full-duplex (IFD) realization, and cellular IoT system. He performed the standardization activities of 3GPP LTE (2005–2007) and IEEE 802.11ad (2009–2010), developing the prototype of IFD system (2014–2015). Dr Chang was the recipient of the Brain Korea Scholarship, during his PhD. He was the recipient of the Certificate of Appreciation, the Day of the Inventions, and the Best Patent Award, from IEEE 802.11ad (2012), Korean Ministry of Commerce, Industry and Energy (2018), and ETRI (2019), respectively.

Young-Jo Ko received the BS, MS, and PhD degrees in Physics from Korea Advanced Institute of Science and Technology, Daejeon, Republic of Korea, in 1992, 1994, and 1998, respectively. He joined Electronics and Telecommunications Research Institute (ETRI) in March, 1998. Since 2002, he has been working on mobile communications at ETRI. From 2005 to 2014, he participated in the development of early versions of LTE/LTE-Advanced systems and also participated in the 3GPP standardization of LTE/LTE-Advanced as a main delegate of ETRI. He is currently director of the 6G Wireless Technology Research Section in Mobile Communication Research Division at ETRI and serves as chairman of the Technology Committee of 5G Forum in Korea. His research interests, in recent years, include 5G New Radio and beyond, and 6G technologies, with his main focus lying in the physical layer aspects of radio access.